microOMEGAs4.1: two dark matter candidates

G. Bélanger[1], F. Boudjema[1], A. Pukhov[2], A. Semenov[3]

1) LAPTH, Univ. de Savoie, CNRS, B.P.110, F-74941 Annecy-le-Vieux, France
2) Skobeltsyn Inst. of Nuclear Physics, Moscow State Univ., Moscow 119992, Russia
3) Joint Institute of Nuclear research, JINR, 141980 Dubna, Russia

Abstract

`microOMEGAs` is a code to compute dark matter observables in generic extensions of the standard model. This version of `microOMEGAs` includes a generalization of the Boltzmann equations to take into account the possibility of two dark matter candidates. The modification of the relic density calculation to include interactions between the two DM sectors as well as semi-annihilation is presented. Both DM signals in direct and indirect detection are computed as well. An extension of the standard model with two scalar doublets and a singlet is used as an example.

1   Introduction

Strong evidence for dark matter at the scale of galaxies and galaxy clusters is sustained by recent precise cosmological observations by the PLANCK satellite [1]. However, the simplest WIMP paradigm, e.g. within the framework of SUSY, is challenged by collider data since no evidence for new particles was found in the first LHC run [2, 3]. At the same time several anomalies have been observed in both direct detection [4, 5, 6, 7, 8] and indirect detection experiments [9, 10, 11, 12]. The various signals corresponding to vastly different mass scales cannot be explained by a single dark matter candidate. Moreover some of these anomalies hint at cross sections stronger than the canonical value deduced from cosmological observations. While these anomalies cannot be unambiguously associated with dark matter, for example pulsars could be the source of the higher than expected positron flux at high energies [13], and anomalies in direct detection corresponding to light dark matter are challenged by competing experiments with null results [14, 15], these observations raise the interesting possibility that the anomalies could be due to two dark matter candidates.

On the theoretical side, multi-component DM models have been considered a long time ago. For example the idea that the neutrino, the axion or its supersymmetric partner, the axino could constitute a fraction of the total DM has been examined carefully over the years [16, 17, 18, 19]. Models where both components are WIMPs - and could therefore lead to typical signatures at different mass scales - have also been examined [20, 21, 22, 23, 24, 25, 26, 27, 28, 29, 30, 31, 32, 33, 34].

When DM is made of two WIMPs the interactions between the two dark matter - so-called dark matter conversion [35, 36], modify the Boltzmann equation and impact the computation of the relic density. Here we generalize the `microOMEGAs` routine to compute the relic density to include all possible interactions between the particles in the dark sectors. In particular all semi-annihilation processes (where two dark matter particles annihilate into another dark matter particle and a standard one) are also included. We also add a few facilities to the direct and indirect detection routines to take into account

the contribution of each component to the DM density. As a working example of a multi-component DM model we consider an extension of the SM containing one extra scalar doublet and one scalar singlet. A Z_4 discrete symmetry leads to two stable DM candidates and implies both semi-annihilations and self-interactions between the two dark sectors [24, 34].

This paper is organized as follows. In section 2 we list all possible DM interactions and mention the Z_N or $Z_N \times Z_M$ discrete groups that could lead to these interactions. The generalization of the relic density calculation and the method used to solve these equations are described in section 3. The modification of the micrOMEGAs routines that deal with two DM candidates are described in section 4. Section 5 contains sample results obtained for the Z_4 model with two doublets and a singlet.

2 Classification of 2-DM models.

micrOMEGAs exploits the fact that models of dark matter exhibit a discrete symmetry and that the fields of the model transform as

$$\phi \rightarrow e^{i2\pi X_\phi} \phi \tag{1}$$

where the charge $|X_\phi| < 1$.

The particles of the Standard Model are assumed to transform trivially under the discrete symmetry, $X_\phi = 0$. The lightest particle with charge $X_\phi \neq 0$ will be stable and, if neutral, can be considered as a DM candidate. Typical examples of discrete symmetries used for constructing single DM models are Z_2 and Z_3. Multi-component DM can arise in models with larger discrete symmetries. A simple example is a model with $Z_2 \times Z_2'$ symmetry, the particles charged under $Z_2(Z_2')$ will belong to the first (second) dark sector. The lightest particle of each sector - whether it is a fermion or a scalar - will be stable and therefore a potential DM candidate. Another example is a model with a Z_4 symmetry. The two dark sectors contain particles with $X_\phi = \pm 1/4$ and $X_\phi = 1/2$ respectively. The lightest particle with charge $1/4$ is always stable while the lightest particle of charge $1/2$ is stable only if its decay into two particles of charge $1/4$ is kinematically forbidden,

We can write all possible dimension-4 interactions for models with two dark sectors. Let ϕ_a and ϕ_b be the generic names of particles belonging to each dark sector, with $X_a \neq \pm X_b \neq 0$. For any choice of discrete group, the potential for scalars can contain the terms [1]

$$V_0 = m_a^2 \phi_a \bar{\phi}_a + m_b^2 \phi_b \bar{\phi}_b + \lambda_a \phi_a^2 \bar{\phi}_a^2 + \lambda_b \phi_b^2 \bar{\phi}_b^2 + \lambda_{ab} \phi_a \bar{\phi}_a \phi_b \bar{\phi}_b \tag{2}$$

Here we omit isospin indices and assume that $\phi_a(\phi_b)$ represent all the different scalar particles with a given discrete charge. Additional terms are possible depending on the choice of the symmetry group. The list of all possible structures for models with two scalar dark sectors is given in Table 2 together with the lowest Z_N or $Z_N \times Z_M$ symmetry that leads to such interactions. When the dark sector contains fermions and gauge bosons, the number of allowed terms is more limited and can be easily written for each specific case.

---

[1] We do not write the generic Lagrangians when the dark sector contains fermions and gauge bosons, this Lagrangian is simpler than for scalars and can be easily adapted for each choice of symmetry and particle content.

title	terms	group	X_a	X_b
L2x2	$\phi_a^2 + \phi_a^4 + \phi_b^2 + \phi_b^4 + \phi_a^2\phi_b^2 + \bar{\phi}_a^2\phi_b^2$	$Z_2 \times Z_2$	$k/2$	$n/2$
L3x3	$\phi_a^3 + \phi_b^3$	$Z_3 \times Z_3$	$k/3$	$n/3$
L2x3	$\phi_a^2 + \phi_a^4 + \phi_b^3$	$Z_2 \times Z_3$	$k/2$	$n/3$
L4	$\phi_a^2\phi_b + \phi_a^4 + \phi_b^2 + \phi_b^4 + \phi_a^2\bar{\phi}_b$	Z_4	$k/4$	$-k/2$
L5	$\phi_a^3\phi_b + \phi_a^2\bar{\phi}_b + \phi_b^3\bar{\phi}_a + \phi_a\phi_b^2$	Z_5	$k/5$	$-3k/5$
L6a	$\phi_a^2\phi_b + \phi_b^3 + \bar{\phi}_a^2\phi_b^2$	Z_6	$k/3 + n/2$	$k/3$
L6b	$\phi_a^3\phi_b + \phi_b^2 + \phi_b^4 + \phi_a^3\bar{\phi}_b$	Z_6	$k/6$	$-k/2$
L7	$\phi_a^2\phi_b + \bar{\phi}_a\phi_b^3$	Z_7	$3k/7$	$k/7$
L8a	$\phi_a^2\phi_b + \phi_b^4$	Z_8	$-k/8$	$k/4$
L8b	$\phi_a\phi_b^3 + \phi_a^3\phi_b + \bar{\phi}_a^2\phi_b^2$	Z_8	$-3k/8$	$k/8$
L9	$\phi_a^3\phi_b + \phi_b^3$	Z_9	$k/9$	$-2k/3$
L12	$\phi_a^3\phi_b + \phi_b^4$	Z_{12}	$k/12$	$-k/4$

Table 1: Table of generic group structures and interaction vertices for 2-component DM models, here k, n are integers. Hermitian conjugated terms are omitted, the complete list can be obtained swapping $\phi_a \leftrightarrow \bar{\phi}_a$ and $\phi_a \leftrightarrow \phi_b$.

The Lagrangian for a concrete multi-component DM model will of course depend on the spin and isospin of the non-standard particles. Consider a model with two scalar doublets H_1 and H_2 and a singlet, S. We impose a Z_4 symmetry with $X_{H_1} = 0$, $X_{H_2} = 1/2$ and $X_S = 1/4$. Both H_2 and S are inert, i.e. they do not couple to fermions while H_1 has couplings similar to those of the SM Higgs, for more details see Ref. [24]. The field ϕ_a stands for the singlet and ϕ_b with the doublet. The potential reads

$$
\begin{aligned}
V_{Z_4} = V_0 &+ \frac{\lambda_S}{2}(S^4 + S^{\dagger 4}) + \frac{\lambda_5}{2}\left[(H_1^\dagger H_2)^2 + (H_2^\dagger H_1)^2\right] \\
&+ \frac{\lambda_{S12}}{2}(S^2 H_1^\dagger H_2 + S^{\dagger 2} H_2^\dagger H_1) + \frac{\lambda_{S21}}{2}(S^2 H_2^\dagger H_1 + S^{\dagger 2} H_1^\dagger H_2),
\end{aligned}
\tag{3}
$$

where

$$
\begin{aligned}
V_0 = &\mu_1^2|H_1{}^2| + \lambda_1|H_1{}^4| + \mu_2^2|H_2|^2 + \lambda_2|H_2|^4 + \mu_S^2|S|^2 + \lambda_S|S|^4 \\
&+ \lambda_{S1}|S|^2|H_1|^2 + \lambda_{S2}|S|^2|H_2|^2 + \lambda_3|H_1|^2|H_2|^2 + \lambda_4(H_1^\dagger H_2)(H_2^\dagger H_1).
\end{aligned}
\tag{4}
$$

.

3 Relic density computation

3.1 Evolution equations

The derivation of the equations for the number density of two DM particles is based on standard assumptions: 1) all particles of the same sector are in thermal equilibrium b) particles of the dark sectors have the same kinetic temperature as those of the SM c) the number densities of DM particles can differ from the equilibrium values when the number density of DM particles times their annihilation cross section becomes too low to

keep up with the expansion rate of the Universe. The different processes that influence the number densities of DM include the annihilation and co-annihilation processes in each sector $\phi_\alpha \phi_\alpha^* \to XX$, the DM conversion processes $\phi_\alpha \phi_\beta \to \phi_\gamma \phi_\delta$, and the semi-annihilation processes $\phi_\alpha \phi_\beta \to \phi_\gamma X$. Here X denotes any SM particle and ϕ_α stands for any particle in the dark sectors. The equation for the number densities, n_a of DM particles in sector 1 and 2 reads

$$
\begin{aligned}
\frac{dn_a}{dt} = & -\sigma_v^{aa00}\left(n_a^2 - \bar{n}_a^2\right) - \sigma_v^{aab0}\left(n_a^2 - n_b\frac{\bar{n}_a^2}{\bar{n}_b}\right) - \sigma_v^{aabb}\left(n_a^2 - n_b^2\frac{\bar{n}_a^2}{\bar{n}_b^2}\right) \\
& -\frac{1}{2}\sigma_v^{aaa0}\left(n_a^2 - \bar{n}_a n_a\right) - \frac{1}{2}\sigma_v^{aaab}\left(n_a^2 - n_a n_b\frac{\bar{n}_a}{\bar{n}_b}\right) - \frac{1}{2}\sigma_v^{abbb}\left(n_a n_b - n_b^2\frac{\bar{n}_a}{\bar{n}_b}\right) \\
& -\frac{1}{2}\sigma_v^{abb0}\left(n_a n_b - n_b\bar{n}_a\right) + \frac{1}{2}\sigma_v^{bba0}(n_b^2 - n_a\frac{\bar{n}_b^2}{\bar{n}_a}) - 3Hn_a
\end{aligned}
\tag{5}
$$

Here b denotes DM sector different from a ($a \neq b$), $\bar{n}_a$ and $\bar{n}_b$ denote the equilibrium number densities of particles in the two dark sectors. The label 0 is used for SM particles, σ_v^{abcd} means the thermally averaged cross section defined as

$$
\sigma_v^{abcd}(T) = \frac{T}{8\pi^4 \overline{n}_a(T)\overline{n}_b(T)} \int ds\sqrt{s}K_1\left(\frac{\sqrt{s}}{T}\right) \sum_{\substack{\alpha\in a \ \beta\in b \\ \gamma\in c \ \delta\in d \\ \text{pol.}}} p_{\alpha\beta}^2(s)\sigma_{\alpha\beta\to\gamma\delta}(s),
\tag{6}
$$

$$
\overline{n}_a(T) = \frac{T}{2\pi^2} \sum_{\alpha\in a} g_\alpha m_\alpha^2 K_2(\frac{m_\alpha}{T}),
\tag{7}
$$

Here $\sigma_{\alpha\beta\to\gamma\delta}$ is the cross section for the process $\phi_\alpha \phi_\beta \to \phi_\gamma \phi_\delta$, K_1, K_2 are modified Bessel functions of the second kind, and m_α and g_α stand for the mass and the number of degrees of freedom of particle ϕ_α. Roman indices take the value $0, 1, 2$ and Greek indices are used to designate particles in a given sector. The inverse reactions are related via the detailed balance equation

$$
\bar{n}_a \bar{n}_b \sigma_v^{abcd} = \bar{n}_c \bar{n}_d \sigma_v^{cdab}.
\tag{8}
$$

Note that in a particular model, only a subset of all possible $2 \to 2$ processes for DM annihilation listed in Table 2 will be allowed, and only the relevant terms will be included in Eq. 5 by `micrOMEGAs`.[2]

Usually the DM evolution equations are solved in terms of the abundance, $Y_a = n_a/s$, where s is the entropy density. The equation for entropy conservation

$$
\frac{ds}{dt} = -3Hs
\tag{9}
$$

allows to convert the time evolution equation into an evolution with respect to the entropy density. Introducing $\Delta Y_a = Y_a - \overline{Y}_a = \frac{n_a - \bar{n}_a}{s}$, Eq. (5) takes the simple form

$$
3H\frac{d\Delta Y_a}{ds} = -C_a + A_{ab}(s)\Delta Y_b + Q_{abc}(s)\Delta Y_b \Delta Y_c,
\tag{10}
$$

---

[2]Note that 3-body final states from virtual W and Z exchange are also included in the annihilation (coannihilation) processes entering the thermally averaged cross section by setting the switches VWdecay,VZdecay =1(2).

where

$$C_a = 3H\frac{d\overline{Y}_a}{ds}, \tag{11}$$

$$A_{aa} = \overline{Y}_a(2(\sigma_v^{aa00} + \sigma_v^{aab0} + \sigma_v^{aabb}) + \frac{1}{2}(\sigma_v^{aaa0} + \sigma_v^{aaab}))$$

$$+ \frac{1}{2}\overline{Y}_b(\sigma_v^{abb0} + \sigma_v^{abbb} + \frac{\overline{Y}_b}{\overline{Y}_a}\sigma_v^{bba0}) \tag{12}$$

$$A_{ab} = -\overline{Y}_a(\frac{1}{2}\sigma_v^{abaa} + \frac{1}{2}\sigma_v^{abbb} + \overline{Y}_a/\overline{Y}_b\sigma_v^{aab0}) - \overline{Y}_b(2\sigma_v^{bbaa} + \sigma_v^{bba0}) \tag{13}$$

$$Q_{aaa} = \sigma_v^{aa00} + \sigma_v^{aab0} + \sigma_v^{aabb} + \frac{1}{2}(\sigma_v^{aaa0} + \sigma_v^{aaab}) \tag{14}$$

$$Q_{aab} = \frac{1}{2}(\sigma_v^{abbb} + \sigma_v^{abb0} - \sigma_v^{abaa}) \tag{15}$$

$$Q_{aba} = 0 \tag{16}$$

$$Q_{abb} = -\sigma_v^{bbaa} - \frac{1}{2}\sigma_v^{bbab} - \frac{1}{2}\sigma_v^{bba0} \tag{17}$$

Here as above $b \neq a$. Since s is a known function of temperature T, Eq. (10) is actually the temperature evolution equation.

3.2 Solution of equations

At temperatures larger than the masses of DM particles $\overline{Y}_a$ is constant and represents the fraction of total degrees of freedom for each dark sector. Since it is constant, $C_a = 0$, and the solution of Eq.(10) is $\Delta Y_a = 0$, which means that the DM particles are in thermal equilibrium with SM particles. Note that we make the approximation that $\Delta Y \leq \overline{Y}$ such that terms in $\Delta Y_j \Delta Y_k$ in Eq.(10) are neglected. Small deviations from equilibrium are obtained by solving

$$\Delta Y(s) = A^{-1}(s)C(s). \tag{18}$$

The numerical solution of Eq. 10 used in the case of one component DM needs to be adapted, the problem is caused by a very small step size in the integration routine. In the region where the linear term dominates, the step of the integration over $\log(s)$ is about $H/(sA)$ leading to a very small step size when $T \approx M_{cdm}$. To bypass this problem in the one component DM case, we used the approximation (18) until

$$\Delta Y_i \approx 10^{-2}\overline{Y} \tag{19}$$

At this point we switch to the numerical solution using the standard Runge-Kutta method. For two components DM, the matrix A_{ij} has two eigenstates. When there is a noticeable mass difference between the two DM particles, the freeze-out of the heavy component occurs much before that of the light one. Thus we have a region of temperatures where the approximation (18) does not apply because the eigenvalue of one of the eigenstate of A is small, however the direct numerical integration stalls because the large eigenvalue forces a very small step of integration. In fact it means that the space of solutions has an attractor line. Equations which pose such numerical problems are known as *stiff* equations. To solve such equations the *backward* scheme is used. In this scheme at each

step of integration one evaluates derivatives at the final point of the step rather than at the initial point as in the standard scheme. In `micrOMEGAs` we use the Rosenbrock algorithm [37, 38] for solving stiff equations. This method finds a solution for points where the standard Runge-Kutta method fails. In the current version we use the Fortran code presented in [38].

To speed up the calculation we first tabulate different cross sections as a function of the temperature in the interval $T \in [\text{Tend}, \text{Tstart}]$, where Tstart is the temperature for which the condition Eq. 19 is satisfied after solving Eq. 18, and Tend $= 10^{-3}$GeV. Functions which interpolates the tabulated data are accessible to the user after the calculation of the relic density. These functions have the generic name $\text{vs}ijkl\text{F(T)}$ where i, j, k, l can take the value $0,1,2$ and $0 < i \leq j$, $k \geq l$. The temperature dependence of the equilibrium abundances can also be called by the user, the functions are named Y_1(T) and Y_2(T) and are defined only in the interval $T \in [\text{Tend}, \text{Tstart}]$.

4 Two DM models in micrOMEGAs

In previous versions of `micrOMEGAs` [39, 40] we assumed that the names of all particles transforming non-trivially under the discrete symmetry group started with '~'. In the current version we need to distinguish the particles with different transformation properties with respect to the discrete group, that is particles belonging to different 'dark' sectors. For this we use the convention that the names of particles in the second 'dark' sector starts with '~~'. Note that `micrOMEGAs` does not check the symmetry of the Lagrangian, it assumes that the name convention correctly identifies all particles with the same discrete symmetry quantum numbers.

Before evaluating DM observables in `micrOMEGAs` one needs to call the initialization routine

• `sortOddParticles(name)`

which fills the global parameters presented in Table 2. Note that there is no restriction on

Table 2: Evaluated global variables

Name	units	comments
CDM1	*character*	name of the lightest particle in first DM sector
CDM2	*character*	name of the lightest particle in second DM sector
Mcdm1	GeV	Mass of CDM1
Mcdm2	GeV	Mass of CDM2
Mcdm	GeV	$\min(Mcdm1, Mcdm2)$ if both exist

the relative values of `Mcdm1` and `Mcdm2`, either can be the lightest one. This micromegas4.X version also works for models with only one DM candidate. In this case `CDM1` or `CDM2` (depending on the name convention chosen by the user) will be initialized by NULL in C and a blank string in Fortran. The corresponding mass will be set to zero. The return parameter *name* contains the name of the lightest particle and `Mcdm` its mass. If `micrOMEGAs` gets NAN while evaluating constraints, then *name* contains the name of the problematic constraint and `sortOddParticles` returns an error code.

There are two functions for the evaluation of the relic density. The new routine

●darkOmega2(fast, Beps)

calculates Ωh^2 for both one- and two-components DM models. The parameter fast=1 flag forces the fast calculation (for more details see Ref. [39]). This is the recommended option and gives an accuracy around 1%. The parameter Beps defines the criteria for including a given coannihilation channel in the computation of the thermally averaged cross-section, [39]. The recommended value is Beps=$10^{-4} - 10^{-6}$, if Beps= 1 only annihilation of the lightest odd particle is computed. darkOmega2 also calculates the global parameter fracCDM2 which represents the mass fraction of CDM2 in the total relic density

$$\Omega = \Omega_1 + \Omega_2 \qquad (20)$$

$$\texttt{fracCDM2} = \frac{\Omega_2}{\Omega} \qquad (21)$$

This parameter is then used in routines which calculate the total signal from both DM candidates in direct, indirect and neutrino telescope experiments, nucleusRecoil, calcSpectrum, and neutrinoFlux. The user can change the global fracCDM2 parameter before the calculation of these observables to take into account the fact that the value of the dark matter fraction in the Milky Way could be different than in the early Universe.

The darkOmega function is the same as in previous versions and is appropriate for models with only one dark matter candidate since it does not distinguish the classes of the discrete symmetry group. For example it will assume that all particles whose name starts with one or two tildes belong to the same dark sector and are in thermal equilibrium. This is in general not the case if the discrete symmetry distinguishes two dark matter sectors. The darkOmega function should therefore be used only for models with one dark matter sector.

The DM nucleon amplitude and cross section relevant for direct detection is computed for each DM candidate with the help of the routine

● nucleonAmplitudes(CDM, qBOX,pAsi,pAsd,nAsi,nAsd)

where the first parameter is the name of DM particles. All other parameters have the same meaning as in previous versions. Here there is no rescaling to account for the dark matter fraction of each component.

The micrOMEGAs routines for model independent analyses contained in the mdlIndep directory do not take into account the possibility of two DM particles. These routines depend only on the global parameter Mcdm. All facilities of previous versions of micrOMEGAs [41] are included in this version except for the option to compute the relic density and DM observables when there is an initial DM $-\overline{\text{DM}}$ asymmetry. A complete list of micrOMEGAs routines is provided in the manual contained in the man directory.

5 Example

As an example we will consider an extension of the SM with two Higgs doublets and a singlet and a discrete Z_4 symmetry [34]. The potential of the model is given in Eqs. (4, 3), the independent parameters are chosen as the masses of the scalars $M_h, M_H, M_S, M_{H^0}, M_{A^0}$ and 8 of the λ_i's, see Table 3. The first dark sector contains only S while the dark sector 2 contains the doublet $H_0, A^0, H^\pm$, with either H^0 or A^0 as the possible dark matter. For the set of input parameters defined in Table 3, The evolution of the abundance for the

two dark matter candidates S, H is illustrated in Figure 5. Furthermore the abundances are compared with the case where DM conversion and/or semi-annihilation is ignored.

Table 3: Input parameters of Z_4 model

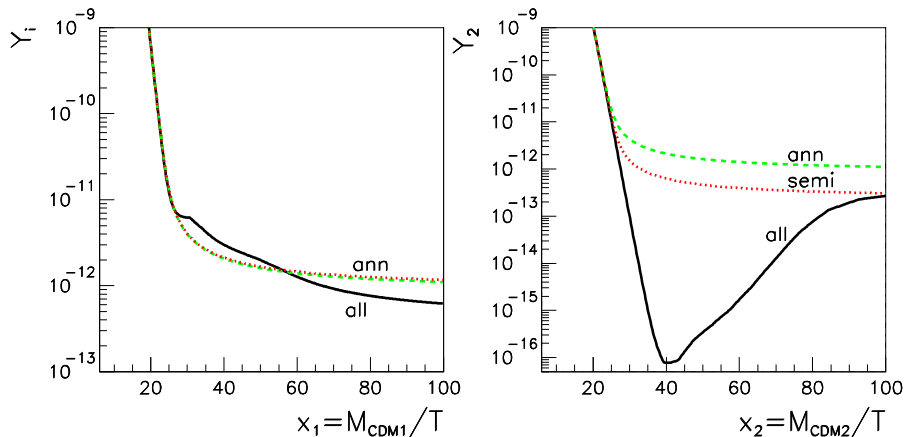| Name	Value		Name	Value		Name	Value	
Mh	125.89	m_h	la2	0.8162	λ_2	laS1	0.2367	λ_{S_1}
Msc	578.0	m_s	la3	-0.1723	λ_3	laS2	-1.139	λ_{S_2}
MHX	895.5	m_H	laS	1.9121	λ_S	laS12	0.7629	$\lambda_{S_{12}}$
MH3	900.6	m_A	lapS	1.017	λ'_S	laS21	-0.2054	$\lambda_{S_{21}}$
MHC	895.64	m_{H+}						

Figure 1: Abundance (Y_i) as a function of $x = M_{\text{CDM1}}/T$ for each DM particle in the doublet and singlet Z_4 model when including all channels (full), only annihilation channels (dash), and also semi-annihilation channels (dot). Note that for CDM1 (left plot), adding semi-annihilation channels induces only a few percent variation in the abundance.

Running `micrOMEGAs` for the benchmark point of Table 3 (benchn3.par) with the options `MASSES_INFO,OMEGA`, `INDIRECT_DETECTION,DIRECT_DETECTION` and the switches `VWDECAY=1,VZDECAY=1` will lead to the following output

```
Dark matter candidate is '~sc' with spin=0/2 mass=5.78E+02
Dark matter candidate is '~~X' with spin=0/2 mass=8.96E+02

=== MASSES OF HIGG AND ODD PARTICLES: ===
Higgs masses and widths
      h   125.89 4.26E-03


Masses of odd sector Particles:
~sc  : Msc  =    578.0 || ~~X : MHX   =    895.5 || ~~H+ : MHC   =    895.6
~~H3 : MH3  =    900.6 ||
```

```
==== Calculation of relic density =====
omega1=5.91E-02
omega2=6.14E-02


==== Indirect detection =======
    Channel           vcs[cm^3/s]
=================================
 annihilation cross section 5.89E-26 cm^3/s
 contribution of processes
 annihilation cross section 5.89E-26 cm^3/s
 contribution of processes
  ~sc,~~X -> Z ~Sc       1.83E-01
  ~Sc,~~X -> Z ~sc       1.83E-01
  ~~X,~~X -> W+ W-       7.47E-02
  ~sc,~sc -> W- ~~H+      7.24E-02
  ~Sc,~Sc -> W+ ~~H-      7.24E-02
  ~sc,~~X -> h ~Sc       6.15E-02
  ~Sc,~~X -> h ~sc       6.15E-02
  ~~X,~~X -> Z Z         5.20E-02
  ~sc,~Sc -> W+ W-       3.95E-02
  ~sc,~sc -> Z ~~X       2.82E-02
  ~Sc,~Sc -> Z ~~X       2.82E-02
  ~sc,~sc -> h ~~H3      2.30E-02
  ~Sc,~Sc -> h ~~H3      2.30E-02
  ~sc,~Sc -> Z Z         1.96E-02
  ~sc,~Sc -> h h         1.91E-02
  ~~X,~~X -> h h         1.09E-02
  ~sc,~sc -> Z ~~H3      8.50E-03
  ~Sc,~Sc -> Z ~~H3      8.50E-03
  ~sc,~sc -> h ~~X       7.27E-03
  ~Sc,~Sc -> h ~~X       7.27E-03
  ~sc,~sc -> W+ ~~H-      5.57E-03
  ~Sc,~Sc -> W- ~~H+      5.57E-03
  ~sc,~Sc -> t T         3.85E-03
  ~~X,~~X -> t T         8.32E-04
sigmav=5.89E-26[cm^3/s]
Photon flux  for angle of sight f=0.10[rad]
and spherical region described by cone with angle 0.10[rad]
Photon flux = 2.13E-16[cm^2 s GeV]^{-1} for E=289.0[GeV]
Positron flux  =  1.01E-14[cm^2 sr s GeV]^{-1} for E=289.0[GeV]
Antiproton flux  =  1.75E-13[cm^2 sr s GeV]^{-1} for E=289.0[GeV]


==== Calculation of CDM-nucleons amplitudes  =====
CDM[antiCDM]-nucleon micrOMEGAs amplitudes for ~sc
proton:  SI  1.813E-09 [1.813E-09]  SD  0.000E+00 [0.000E+00]
neutron: SI  1.831E-09 [1.831E-09]  SD  0.000E+00 [0.000E+00]
```

```
CDM[antiCDM]-nucleon cross sections[pb]:
 proton  SI 1.433E-09 [1.433E-09] SD 0.000E+00 [0.000E+00]
 neutron SI 1.461E-09 [1.461E-09] SD 0.000E+00 [0.000E+00]
CDM[antiCDM]-nucleon micrOMEGAs amplitudes for ~~X
proton:  SI  -8.929E-10 [-8.929E-10]  SD  0.000E+00 [0.000E+00]
neutron: SI  -9.017E-10 [-9.017E-10]  SD  0.000E+00 [0.000E+00]
CDM[antiCDM]-nucleon cross sections[pb]:
 proton  SI 3.473E-10 [3.473E-10] SD 0.000E+00 [0.000E+00]
 neutron SI 3.543E-10 [3.543E-10] SD 0.000E+00 [0.000E+00]
```

Acknowledgements

Appendix

As another example of a two-component DM model, we consider a model that contains two singlets S_1 and S_2 in addition to the SM Higgs doublet, H. We impose a Z_5 discrete symmetry with $X_H = 0$, $X_{S_1} = 1/5$ and $X_{S_2} = -3/5$. The potential reads

$$
\begin{aligned}
V_{Z_5} = V_0 &+ \frac{\lambda_{31}}{2}(S_1^3 S_2 + S_1^{\dagger 3} S_2^{\dagger}) + \frac{\lambda_{32}}{2}(S_2^3 S_1^{\dagger} + S_2^{\dagger 3} S_1) \\
&+ \frac{\mu_{SS1}}{2}(S_1^2 S_2^{\dagger} + S_1^{\dagger 2} S_2) + \frac{\mu_{SS2}}{2}(S_1 S_2^2 + S_1^{\dagger} S_2^{\dagger 2}),
\end{aligned}
\tag{22}
$$

where

$$
\begin{aligned}
V_0 = \mu_1^2|H^2| &+ \lambda_1|H^4| + \mu_{S1}^2|S_1|^2 + \mu_{S2}^2|S_2|^2 + \lambda_{41}|S_1|^4 + \lambda_{42}|S_2|^4 + \lambda_{412}|S_1|^2|S_2|^2 \\
&+ \lambda_{S1}|S_1|^2|H|^2 + \lambda_{S2}|S_2|^2|H|^2
\end{aligned}
\tag{23}
$$

is the part of the potential valid for any choice of discrete symmetry Z_N. The input parameters of the model are the masses M_h, M_{S1}, M_{S2} and the couplings $\lambda_{41}, \lambda_{42}, \lambda_{412}, \lambda_{31}, \lambda_{32}, \lambda_{S1}, \lambda_{S2}, \mu_{SS1}, \mu_{SS2}$. This model features only one particle in each of the dark sector and includes interactions between the two dark sectors that were not present in the Z_4 model considered in section 5, for example $S_1 S_1 \rightarrow S_1^{\dagger} S_2^{\dagger}$. This model is provided in the directory Z5M together with the `Lanhep` source code to create the appropriate `CalcHEP` model files.

References

[1] **Planck** Collaboration, P. Ade *et al.*, "Planck 2013 results. XVI. Cosmological parameters," arXiv:1303.5076 [astro-ph.CO].

[2] **ATLAS** Collaboration, "A general search for new phenomena in proton-proton collisions at a centre-of-mass energy of 8 TeV with the ATLAS detector.". ATLAS-CONF-2014-006.

[3] **CMS** Collaboration, "Phenomenological MSSM interpretation of the CMS 7 and 8 TeV results.". CMS-PAS-SUS-13-020.

[4] R. Bernabei *et al.*, "New results from DAMA/LIBRA," *Eur. Phys. J.* **C67** (2010) 39–49, arXiv:1002.1028 [astro-ph.GA].

[5] **CoGeNT collaboration** Collaboration, C. Aalseth *et al.*, "Results from a Search for Light-Mass Dark Matter with a P-type Point Contact Germanium Detector," *Phys.Rev.Lett.* **106** (2011) 131301, arXiv:1002.4703 [astro-ph.CO].

[6] **CoGeNT Collaboration** Collaboration, C. Aalseth *et al.*, "CoGeNT: A Search for Low-Mass Dark Matter using p-type Point Contact Germanium Detectors," *Phys.Rev.* **D88** no. 1, (2013) 012002, arXiv:1208.5737 [astro-ph.CO].

[7] G. Angloher, M. Bauer, I. Bavykina, A. Bento, C. Bucci, *et al.*, "Results from 730 kg days of the CRESST-II Dark Matter Search," *Eur.Phys.J.* **C72** (2012) 1971, arXiv:1109.0702 [astro-ph.CO].

[8] **CDMS Collaboration** Collaboration, R. Agnese *et al.*, "Silicon Detector Dark Matter Results from the Final Exposure of CDMS II," *Phys.Rev.Lett.* **111** (2013) 251301, arXiv:1304.4279 [hep-ex].

[9] C. Weniger, "A Tentative Gamma-Ray Line from Dark Matter Annihilation at the Fermi Large Area Telescope," *JCAP* **1208** (2012) 007, arXiv:1204.2797 [hep-ph].

[10] **Fermi LAT** Collaboration, M. Ackermann *et al.*, "Measurement of separate cosmic-ray electron and positron spectra with the Fermi Large Area Telescope," *Phys.Rev.Lett.* **108** (2012) 011103, arXiv:1109.0521 [astro-ph.HE].

[11] **PAMELA** Collaboration, O. Adriani *et al.*, "An anomalous positron abundance in cosmic rays with energies 1.5-100 GeV," *Nature* **458** (2009) 607–609, arXiv:0810.4995 [astro-ph].

[12] **AMS** Collaboration, M. Aguilar *et al.*, "First Result from the Alpha Magnetic Spectrometer on the International Space Station: Precision Measurement of the Positron Fraction in Primary Cosmic Rays of 0.5-350 GeV," *Phys.Rev.Lett.* **110** (2013) 141102.

[13] D. Hooper, P. Blasi, and P. D. Serpico, "Pulsars as the Sources of High Energy Cosmic Ray Positrons," *JCAP* **0901** (2009) 025, arXiv:0810.1527 [astro-ph].

[14] **XENON100 Collaboration** Collaboration, E. Aprile *et al.*, "Dark Matter Results from 225 Live Days of XENON100 Data," *Phys.Rev.Lett.* **109** (2012) 181301, arXiv:1207.5988 [astro-ph.CO].

[15] **LUX Collaboration** Collaboration, D. Akerib *et al.*, "First results from the LUX dark matter experiment at the Sanford Underground Research Facility," *Phys.Rev.Lett.* **112** (2014) 091303, arXiv:1310.8214 [astro-ph.CO].

[16] S. Hannestad and G. Raffelt, "Cosmological mass limits on neutrinos, axions, and other light particles," *JCAP* **0404** (2004) 008, arXiv:hep-ph/0312154 [hep-ph].

[17] S. Hannestad, A. Mirizzi, G. G. Raffelt, and Y. Y. Wong, "Neutrino and axion hot dark matter bounds after WMAP-7," *JCAP* **1008** (2010) 001, arXiv:1004.0695 [astro-ph.CO].

[18] H. Baer, A. D. Box, and H. Summy, "Mainly axion cold dark matter in the minimal supergravity model," *JHEP* **0908** (2009) 080, arXiv:0906.2595 [hep-ph].

[19] K. J. Bae, H. Baer, and E. J. Chun, "Mixed axion/neutralino dark matter in the SUSY DFSZ axion model," *JCAP* **1312** (2013) 028, arXiv:1309.5365 [hep-ph].

[20] E. Ma, "Verifiable radiative seesaw mechanism of neutrino mass and dark matter," *Phys.Rev.* **D73** (2006) 077301, arXiv:hep-ph/0601225 [hep-ph].

[21] K. M. Zurek, "Multi-Component Dark Matter," *Phys.Rev.* **D79** (2009) 115002, arXiv:0811.4429 [hep-ph].

[22] B. Batell, "Dark Discrete Gauge Symmetries," *Phys.Rev.* **D83** (2011) 035006, arXiv:1007.0045 [hep-ph].

[23] H. Fukuoka, D. Suematsu, and T. Toma, "Signals of dark matter in a supersymmetric two dark matter model," *JCAP* **1107** (2011) 001, arXiv:1012.4007 [hep-ph].

[24] G. Bélanger, K. Kannike, A. Pukhov, and M. Raidal, "Impact of semi-annihilations on dark matter phenomenology - an example of Z_N symmetric scalar dark matter," *JCAP* **04** (2012) 010, arXiv:1202.2962 [hep-ph].

[25] M. Aoki, M. Duerr, J. Kubo, and H. Takano, "Multi-Component Dark Matter Systems and Their Observation Prospects," *Phys.Rev.* **D86** (2012) 076015, arXiv:1207.3318 [hep-ph].

[26] I. Ivanov and V. Keus, "Z_p scalar dark matter from multi-Higgs-doublet models," *Phys.Rev.* **D86** (2012) 016004, arXiv:1203.3426 [hep-ph].

[27] D. Chialva, P. B. Dev, and A. Mazumdar, "Multiple dark matter scenarios from ubiquitous stringy throats," *Phys.Rev.* **D87** no. 6, (2013) 063522, arXiv:1211.0250 [hep-ph].

[28] J. Heeck and H. Zhang, "Exotic Charges, Multicomponent Dark Matter and Light Sterile Neutrinos," *JHEP* **1305** (2013) 164, arXiv:1211.0538 [hep-ph].

[29] K. P. Modak, D. Majumdar, and S. Rakshit, "A Possible Explanation of Low Energy γ-ray Excess from Galactic Centre and Fermi Bubble by a Dark Matter Model with Two Real Scalars," arXiv:1312.7488 [hep-ph].

[30] M. Aoki, J. Kubo, and H. Takano, "Two-loop radiative seesaw mechanism with multicomponent dark matter explaining the possible ? excess in the Higgs boson decay and at the Fermi LAT," *Phys.Rev.* **D87** no. 11, (2013) 116001, `arXiv:1302.3936 [hep-ph]`.

[31] C.-Q. Geng, D. Huang, and L.-H. Tsai, "Imprint of Multi-component Dark Matter on AMS-02," *Phys.Rev.* **D89** (2014) 055021, `arXiv:1312.0366 [hep-ph]`.

[32] Y. Kajiyama, H. Okada, and T. Toma, "Multicomponent dark matter particles in a two-loop neutrino model," *Phys.Rev.* **D88** no. 1, (2013) 015029, `arXiv:1303.7356`.

[33] S. Bhattacharya, A. Drozd, B. Grzadkowski and J. Wudka, "Two-Component Dark Matter," JHEP **1310** (2013) 158 [`arXiv:1309.2986 [hep-ph]`].

[34] G. Bélanger, K. Kannike, A. Pukhov, and M. Raidal, "Minimal semi-annihilating $\mathbb{Z}_N$ scalar dark matter," *JCAP* **1406** (2014) 021, `arXiv:1403.4960 [hep-ph]`.

[35] Z.-P. Liu, Y.-L. Wu, and Y.-F. Zhou, "Enhancement of dark matter relic density from the late time dark matter conversions," *Eur.Phys.J.* **C71** (2011) 1749, `arXiv:1101.4148 [hep-ph]`.

[36] G. Bélanger and J.-C. Park, "Assisted freeze-out," *JCAP* **1203** (2012) 038, `arXiv:1112.4491 [hep-ph]`.

[37] W. H. Press, S. A. Teukolsky, W. T. Vetterling, and B. P. Flannery, "Numerical recipes in c: The art of scientific computing. second edition," 1992.

[38] G. Hairer, *Solving Ordinary Differential Equations II*. Springer Berlin Heidelberg, 2010.

[39] G. Bélanger, F. Boudjema, A. Pukhov, and A. Semenov, "micrOMEGAs: Version 1.3," *Comput. Phys. Commun.* **174** (2006) 577–604, `arXiv:hep-ph/0405253`.

[40] G. Bélanger, F. Boudjema, A. Pukhov, and A. Semenov, "micrOMEGAs2.0: A program to calculate the relic density of dark matter in a generic model," *Comput. Phys. Commun.* **176** (2007) 367–382, `arXiv:hep-ph/0607059`.

[41] G. Bélanger, F. Boudjema, A. Pukhov, and A. Semenov, "micrOMEGAs3: A program for calculating dark matter observables," *Comput.Phys.Commun.* **185** (2014) 960–985, `arXiv:1305.0237 [hep-ph]`.